Phase relations of some tungstate minerals under hydrothermal conditions

L. C. Hsu

Nevada Bureau of Mines/Geology and
Department of Geological Sciences, Mackay School of Mines
University of Nevada, Reno, Nevada 89557

Abstract

The binary phase relations of several naturally-occurring tungstate minerals, of the general form $M^{2+}WO_4$, were investigated hydrothermally at fluid pressure of 1.0 kbar and temperatures of 400°–900°C. A complete solid solution, with tetragonal symmetry, between scheelite (M^{2+} = Ca) and Stolzite (Pb) forms above 725°C. The solvus is almost symmetrical with a crest near $Ca_{45}Pb_{55}$. The observed linear variation of the 116 interplanar spacing, 1.687(2)Å for Ca to 1.782(2)Å for Pb, may be used to determine composition. Sanmartinite, $(ZnWO_4)$ forms a complete solid solution of monoclinic symmetry with both ferberite ($FeWO_4$), and huebnerite ($MnWO_4$), down to at least 400°C. The interplanar spacing of the 200 reflection of these solid solutions is also observed to vary linearly with composition. Solid solution is very limited between monoclinic and tetragonal tungstates. Less than 5 mole percent miscibility of one in the other is observed at temperatures up to 900°C.

It appears that the solid solution among these tungstate minerals is affected strongly by both the availability and environment of the structural sites for specific divalent cations. Even where structural limitations permit extensive substitution, physicochemical characteristics of elements such as Zn and Pb may still restrict the occurrence of solid solutions in nature.

Introduction

Naturally-occurring tungstate minerals belong to two structural groups. One, including scheelite ($CaWO_4$) and stolzite ($PbWO_4$), crystallizes in the tetragonal system with space group $I4_1/a$; the other, including ferberite ($FeWO_4$), huebnerite ($MnWO_4$) and sanmartinite ($ZnWO_4$), crystallizes in the monoclinic system with space group $P2/c$.

The subsolidus phase relations between scheelite and many other tungstates with divalent cations, except Fe^{2+}, were studied by Chang (1967) at temperatures from 550° to 1150°C under anhydrous atmospheric conditions. He found a complete solid solution between $CaWO_4$ and $PbWO_4$ above 815°C with a broad miscibility gap below that temperature. According to Chang, the system $CaWO_4$–$MnWO_4$ shows extremely low mutual solid solubility; that is, $CaWO_4$ takes up 10 mole percent $MnWO_4$ only at a temperature above 1100°C, whereas $MnWO_4$ takes up only 2.5 mole percent $CaWO_4$ at the same temperature. Yet Grubb (1967) reported that an almost complete solid solution series between wolframite, $(Fe,Mn)WO_4$, and scheelite exists at elevated temperatures, based on his chemical and X-ray diffraction

studies on zoned crystals of ferberitic wolframite containing scheelite inclusions from Australia.

Among the monoclinic tungstate minerals, a complete solid solution series between $FeWO_4$ and $MnWO_4$ has long been known in nature, and Hsu (1976) experimentally demonstrated that the compositional variation of this series in terms of Fe/Mn ratio cannot be used to evaluate temperatures of ore formation. Chang (1968) showed that the solid solubility in the system $MnWO_4$–$ZnWO_4$ is complete above 840°C, below which temperature a broad miscibility gap exists. On the other hand, Chernyshev *et al.* (1976) using hydrothermal techniques determined that no miscibility gaps are observed in the systems $FeWO_4$–$ZnWO_4$ and $MnWO_4$–$ZnWO_4$ at temperature down to 500°C at 1000 atm.

$PbWO_4$ in nature also occurs as the monoclinic mineral, raspite, which has a structure (space group $P2_1/a$) different from other monoclinic tungstate minerals. Raspite is 6 percent denser than stolzite, using data of Fujita *et al.* (1977) for raspite and those of Plakhov *et al.* (1970) for stolzite. Raspite is reported to transform irreversibly to stolzite at 400°C (Shaw and Claringbull, 1955). Raspite has so far defied lab-

oratory synthesis and its relation with stolzite remains unsolved (e.g., Chang, 1971).

The purpose of this investigation was to resolve the above-mentioned conflicting conclusions and, in general, to determine as much as possible about tungstate minerals and mineralization by using conventional hydrothermal techniques and facilities at P–T ranges simulating those involved in natural processes.

Experimental

Conventional hydrothermal techniques were employed throughout the work. All the experiments were made in cold-seal pressure vessels (Tuttle, 1949). Details of the experimental apparatus and P–T calibrations are described elsewhere (Hsu, 1976).

Three tungstate end members, $CaWO_4$, $PbWO_4$ and $ZnWO_4$ were readily prepared by chemical precipitation of reagent grade $Na_2WO_4 \cdot 2H_2O$ solution, respectively, with reagent grade $CaCl_2$, $Pb(NO_3)_2$ and $Zn(NO_3)_2 \cdot 6H_2O$ solutions in stoichiometric proportions. After filtering, washing, and firing these precipitates at 700°C for 24 hours, mixtures of the three binary systems were prepared at 10 mole percent intervals by blending two respective end members. The other two end members $FeWO_4$ and $MnWO_4$ cannot be readily prepared by simple chemical precipitation. Mixtures of these binary systems were prepared by thoroughly mixing reagent grade tungstic acid with respective metal (electrolytic iron and manganese) powders and metal oxides (reagent grade CaO, PbO, and ZnO) stoichiometrically, also at 10 mole percent intervals. Additional mixtures at 5 mole percent intervals were prepared near two end members where necessary.

Each run was sealed in a noble metal capsule with excess distilled water, brought to temperature, and quenched isobarically at a fluid pressure of 1.0 kbar. Whenever necessary, the same run was repeated several times at the same temperature for different periods to ensure equilibrium. Some homogeneous high-temperature products were run at lower temperatures to test whether exsolution had occurred (*e.g.*, Run #5Ca5Pb13).

Condensed run products were examined with a petrographic microscope and a Norelco X-ray diffractometer equipped with a graphite monochromator and scintillation counter and using either CuKα or FeKα radiation. The interplanar spacings were obtained by choosing appropriate internal standards. Three oscillations at $1/4$° 2θ per minute scan speed and $1/2$ in. per minute chart speed were made

for each determination. Measurements were made to 0.005° 2θ and results averaged.

Phase Relations

The subsolidus phase equilibria for nine of the ten possible binary systems were determined at $P_f = 1.0$ kbar and $T = 400$–900°C. These nine systems are Ca–Pb, Fe–Zn, Mn–Zn, Ca–Fe, Ca–Mn, Fe–Pb, Mn–Pb, Ca–Zn, and Pb–Zn. The first three involve end members of the same structure, the rest involve end members of differing structures. Phase relations for the remaining binary system, Fe–Mn, were reported previously (Hsu, 1976).

The system $CaWO_4$–$PbWO_4$.

A complete solid solution between scheelite and stolzite forms above 725°C. The solvus is almost symmetrical with a crest near $Ca_{45}Pb_{55}$. As is shown in Figure 1, the position and shape of the solvus are quite different from those previously found (dotted line) by Chang (1967) under anhydrous, one atmosphere conditions. The difference in the results of the two studies may be attributed principally to the slowness of diffusion and attainment of equilibrium in dry crystalline powders. Here in view of the nature of the starting material being used, hydrous conditions, and the sufficient duration of runs being adopted, equilibrium was considered to be attained. A reversal of reaction was demonstrated by Run #5Ca5Pb13 in which a homogeneous phase formed at higher temperature underwent unmixing, although a still longer run duration is needed as indicated by the measured interplanar spacings.

The intervals between intermediate members plotted in Figure 1 are not 10 mole percent as intended, because a formula weight for $CaWO_4$ of 207.9276 instead of 287.9276 was used accidentally in preparing mixes. This mistake was discovered while plotting the d_{116} values of the two end members and nine intermediate members composition on the binary. Correct mole percent compositions are plotted.

The intensity of the 116 reflection remains consistently high throughout the compositional range. The d_{116} value varies linearly with composition as shown in Figure 2. Using clear natural quartz as an internal standard, with its 112 reflection calibrated against the 220 reflection of Si($a = 4.43012$Å), the d_{116} value was found to vary linearly from 1.687(2)Å for scheelite to 1.782(2)Å for stolzite. The critical runs for this sytem are listed in Table 1.

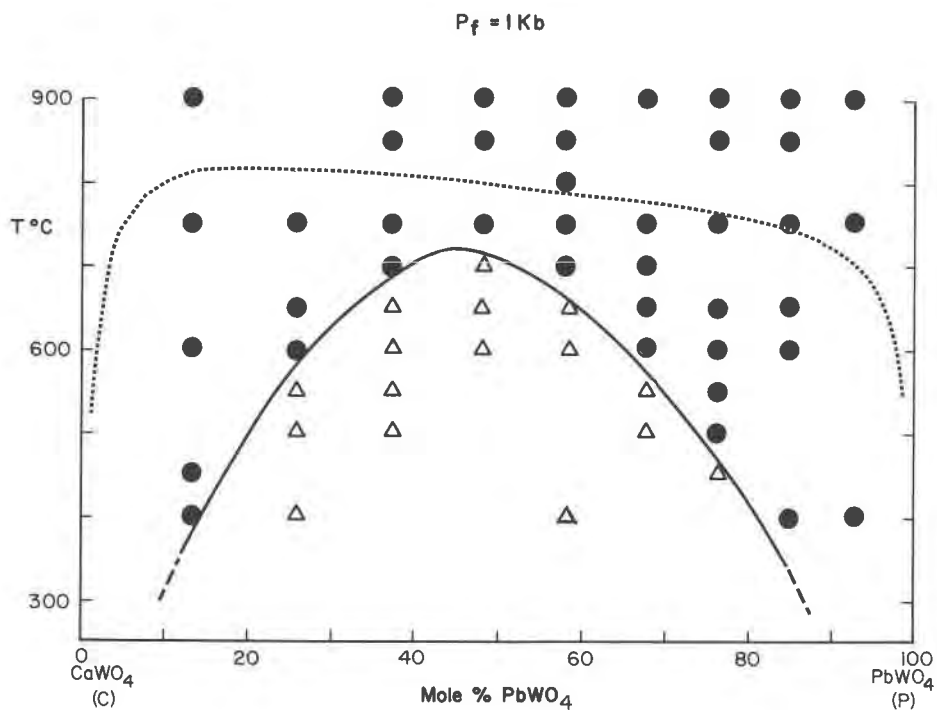Scheelite is the only tungstate mineral which consistently yields a blue to whitish fluorescent color un-

Figure 1. *T–X* diagram at P_f = 1.0 kbar for the Ca–Pb system. Solid circles: single solid solution; open triangles: two solid solutions Dotted line is the solvus after Chang (1967).
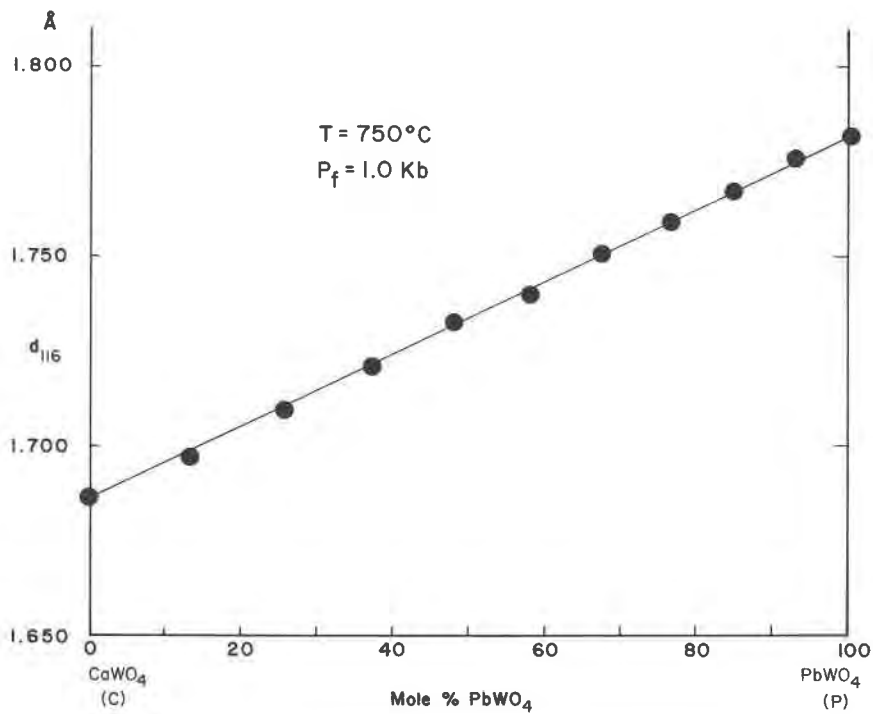

Figure 2. Variation of d_{116} with composition in the Ca–Pb system.

Table 1. Run data for the Ca–Pb system

Run No.	Starting Material	T°C	Duration (days)	Run Product d_{116}Å*
9Ca1Pb2	Tungstate mix	900	2	single solid soln.
9Ca1Pb5	"	750	30	single solid soln., $\underline{d}$ = 1.699
9Ca1Pb8	"	600	30	"
9Ca1Pb12	"	450	72	"
9Ca1Pb1	"	400	86	"
8Ca2Pb7	"	850	4	single solid soln.
8Ca2Pb5	"	750	30	single solid soln., $\underline{d}$ = 1.709
8Ca2Pb9	"	650	40	single solid soln.
8Ca2Pb8	"	600	97	"
8Ca2Pb11	"	550	76	two solid solns., $\underline{d}$ = 1.708, ($\underline{d}$ = 1.752)**
8Ca2Pb3	"	500	83	two solid solns., $\underline{d}$ = 1.704, ($\underline{d}$ = 1.756)
8Ca2Pb1	"	400	113	two solid solns., $\underline{d}$ = 1.699, ($\underline{d}$ = 1.764)
7Ca3Pb2	"	900	6	single solid soln.
7Ca3Pb7	"	850	4	"
7Ca3Pb5	"	750	44	single solid soln., $\underline{d}$ = 1.722
7Ca3Pb10	"	700	72	single solid soln.
7Ca3Pb9	"	650	97	two solid solns.
7Ca3Pb8	"	600	60	two solid solns., $\underline{d}$ = 1.712, ($\underline{d}$ = 1.748)
7Ca3Pb11	"	550	76	two solid solns., $\underline{d}$ = 1.707, ($\underline{d}$ = 1.753)
7Ca3Pb3	"	500	83	two solid solns., $\underline{d}$ = 1.705, $\underline{d}$ = 1.755
6Ca4Pb2	"	900	3	single solid soln.
6Ca4Pb7	"	850	4	"
6Ca4Pb5	"	750	28	single solid soln. $\underline{d}$ = 1.733
6Ca4Pb10	"	700	72	two solid solns., $\underline{d}$ = 1.737, $\underline{d}$ = 1.723
6Ca4Pb9	"	650	97	two solid solns., $\underline{d}$ = 1.717, $\underline{d}$ = 1.745
6Ca4Pb8	"	600	30	two solid solns., $\underline{d}$ = 1.709, $\underline{d}$ = 1.751
5Ca5Pb2	"	900	4	single solid soln.
5Ca5Pb7	"	850	3	"
5Ca5Pb4	"	800	3	"
5Ca5Pb5	"	750	14	single solid soln. $\underline{d}$ = 1.740
5Ca5Pb10	"	700	10	single solid soln.
5Ca5Pb9	"	650	70	two solid solns., $\underline{d}$ = 1.744, $\underline{d}$ = 1.716
5Ca5Pb8	"	600	32	two solid solns.
5Ca5Pb1	"	400	59	two solid solns., $\underline{d}$ = 1.764, $\underline{d}$ = 1.700
5Ca5Pb13	5Ca5Pb2	400	113	three solid solns., $\underline{d}$=1.760, $\underline{d}$=1.739, $\underline{d}$=1.702
4Ca6Pb2	Tungstate mix	900	2	single solid soln.
4Ca6Pb5	"	750	30	single solid soln., $\underline{d}$ = 1.751
4Ca6Pb10	"	700	10	single solid soln.
4Ca6Pb9	"	650	27	"
4Ca6Pb8	"	600	30	single solid soln., $\underline{d}$ = 1.752
4Ca6Pb11	"	550	77	two solid soln., $\underline{d}$ = 1.753, ($\underline{d}$ = 1.707)
4Ca6Pb3	"	500	83	two solid solns., $\underline{d}$ = 1.755, ($\underline{d}$ = 1.705)
3Ca7Pb2	Tungstate mix	900	2	single solid soln.
3Ca7Pb7	"	850	4	"
3Ca7Pb5	"	750	30	single solid soln., $\underline{d}$ = 1.759
3Ca7Pb9	"	650	27	single solid soln.
3Ca7Pb8	"	600	30	"
3Ca7Pb11	"	550	77	"
3Ca7Pb3	"	500	72	"
3Ca7Pb12	"	450	83	two solid solns., $\underline{d}$ = 1.761, ($\underline{d}$ = 1.703)
2Ca8Pb2	"	900	2	single solid soln.
2Ca8Pb7	"	850	4	"
2Ca8Pb5	"	750	30	single solid soln., $\underline{d}$ = 1.767
2Ca8Pb9	"	650	27	single solid soln.
2Ca8Pb8	"	600	30	"
2Ca8Pb1	"	400	86	"
1Ca9Pb2	"	900	2	single solid soln.
1Ca9Pb5	"	750	30	single solid soln., $\underline{d}$ = 1.777
1Ca9Pb8	"	600	30	single solid soln.
1Ca9Pb1	"	400	75	"

*$\underline{d}_{116}$(Å) for pure Ca = 1.687, for pure Pb = 1.782.
**Minor phases are in parenthesis.

der short-wave ultraviolet light. With 2 mole percent $CaMoO_4$ in solid solution, scheelite quickly changes its fluorescent color to yellow and remains essentially so throughout the rest of the solid solution series (Hsu and Galli, 1973), although detailed spectral study enables one to estimate within the accuracy of 1 to 2 mole percent in the range from 0 to 10 mole percent $CaMoO_4$ (Shoji, 1978). In the Ca–Pb series, the fluorescent color changes from bright blue for pure scheelite, through white with a yellowish tint and decreasing brightness for 9Ca1Pb to 7Ca3Pb, to yellowish gray to light gray for 6Ca4Pb and 5Ca5Pb. No fluorescence is observed for the rest of the intermediate members. Pure stolzite fluoresces rather bright yellow when it is well crystallized, but heat-treated chemical precipitate fails to show fluorescence. The fluorescence of stolzite evidently is quickly quenched with minor impurities in the structure, as indicated by the observation that the synthetic stolzite with 3 mole percent $CaWO_4$ (at 750°C, 1 kbar) is no longer fluorescent. Thus the fluorescence behavior of natural stolzite may serve as a good indicator for the chemistry of the mineral. A fluorescence behavior similar to stolzite is also observed for sanmartinite.

The systems $FeWO_4$–$ZnWO_4$ and $MnWO_4$–$ZnWO_4$

From previous study on the wolframite series (Hsu, 1976) it was learned that the d_{200} spacing of the monoclinic tungstate minerals is quite sensitive to compositional variation. By using FeKα radiation the composition of the binary solid solution series can be determined quickly and accurately through measurement of the separation between the 200 reflection of the mineral and the 102 reflection of quartz. The $\Delta 2\theta$ (FeKα) for $FeWO_4$, $MnWO_4$ and $ZnWO_4$ are, respectively, in degrees 1.925(10), 2.920(10), and 1.435(10). As shown in Figure 3, the linear relation between the $\Delta 2\theta$'s and the compositions of the mineral series hold perfectly. A negative deviation from Vegard's rule reported in the Fe–Zn series by Chernyshev *et al.* (1976) is not apparent in the present study. Their usage of the less sensitive, lower order 100 reflection may partly be responsible for this discrepancy. With the d_{102} of quartz calibrated against the d_{110} of spectrochemically pure tungsten powder, the calculated d_{200} for the three end members are 2.3671(5), 2.4140(5), and 2.3448(5)Å, respectively.

A complete solid solution exists for both Fe–Zn and Mn–Zn series (Tables 2, 3), at least down to 400° C at P_f = 1.0 kbar, and perhaps even much lower for
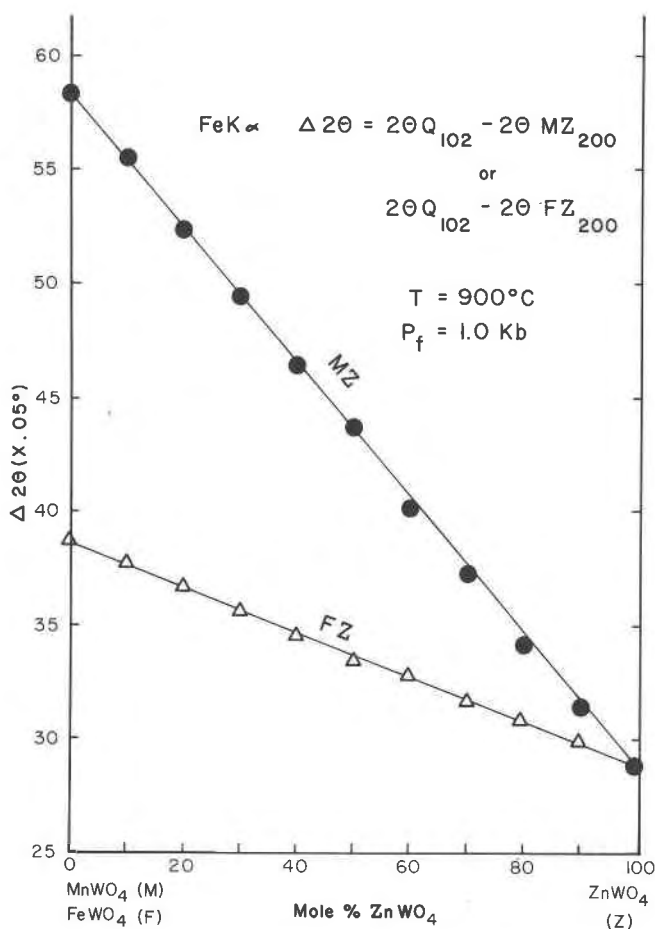
Figure 3. Variation of Δ2Θ with composition in the Fe-Zn and Mn-Zn systems.

the Fe–Zn series. The Mn–Zn series takes much longer to achieve equilibrium and to obtain adequate crystallinity than the Fe–Zn series. In the Mn–Zn series at 400°C, the width of each of the 200 reflections obtained from the products of two-month runs is on the order of twice the width of each of the peaks obtained from the products of four-month or longer runs; peak position remains unchanged, indicating improved crystallinity without compositional change. The higher solvus temperatures reported by previous authors (Chang for Mn–Zn, Cherynshev *et al.,* for Fe–Zn and Mn–Zn) can be attributed simply to kinetics problems.

The systems CaWO₄–FeWO₄, CaWO₄–MnWO₄, FeWO₄–PbWO₄, MnWO₄–PbWO₄, CaWO₄–ZnWO₄, and PbWO₄–ZnWO₄.

Very wide miscibility gaps reported by Chang (1967) in the Ca–Mn and Ca–Zn systems at temper-

atures as high as 1100°C were confirmed in this study. In all the systems, compositions of 5 mole percent one end member with 95 mole percent of the other always produced two-phase assemblages at 900°C. However, within the error of measurement, the interplanar spacings of the products always show a finite but very small change in the proper direction as compared with those of the pure end members. Assuming a linear relation between interplanar spacings and composition allows the solubility limits to be plotted as shown in Figures 4, 5, and 6. The critical runs are listed in Tables 4, 5, and 6. The interplanar spacings, type of X-ray radiation and internal standards employed are included in these tables for each binary system investigated.

Polymorphism of PbWO₄

Chang (1971) attempted to synthesize raspite through chemical precipitation under various pH

Table 2. Run data for the Fe–Zn system

Run No.	Starting Material	T°C	Duration (days)	Run Product Δ2Θ (degrees)*
9Fe1Zn2	Oxide mix	900	3	single solid soln. Δ2Θ = 1.870
9Fe1Zn1	"	400	77	single solid soln.
8Fe2Zn2	"	900	3	single solid soln. Δ2Θ = 1.830
8Fe2Zn1	"	400	77	single solid soln.
7Fe3Zn2	"	900	3	single solid soln. Δ2Θ = 1.780
7Fe3Zn1	"	400	78	single solid soln. Δ2Θ = 1.770
6Fe4Zn2	"	900	6	single solid soln. Δ2Θ = 1.720
5Fe5Zn2	"	900	10	single solid soln. Δ2Θ = 1.670
5Fe5Zn8	"	850	4	single solid soln.
5Fe5Zn6	5Fe5Zn2	700	12	single solid soln.
5Fe5Zn16	Oxide mix	650	110	"
5Fe5Zn13	"	550	142	"
5Fe5Zn10	"	450	180	"
5Fe5Zn1	"	400	188	single solid soln. Δ2Θ = 1.675
4F36Zn2	"	900	6	single solid soln. Δ2Θ = 1.635
3F37Zn2	"	900	3	single solid soln. Δ2Θ = 1.583
3Fe7Zn1	"	400	77	single solid soln. Δ2Θ = 1.580
2Fe8Zn2	"	900	3	single solid soln. Δ2Θ = 1.540
2Fe821	"	400	77	single solid soln.
1F39Zn2	"	900	3	single solid soln. Δ2Θ = 1.490
1Fe9Zn1	"	400	78	single solid soln.

*Δ2Θ FeKα (102 of quartz and 200 of Fe–Zn) for pure Fe = 1.925°; for pure Zn = 1.435°

conditions. Stolzite was produced in all cases. When subjected to high pressure treatment using opposed-anvil apparatus, these precipitates transformed to a high-pressure form of $PbWO_4$. A single crystal of this form was prepared and its structure analyzed later by Richter *et al.* (1976).

In this study, oxide mixes or tungstates from chemical precipitation with seeds of natural raspite or mixtures of natural raspite and stolzite were used as starting material. The natural specimen was from the Cordillera mine, 600 km east of Broken Hill New South Wales, Australia (McColl, 1974) provided through the generosity of D. H. McColl, Museum Curator, Bureau of Mineral Resources, Canberra, Australia. The charges were sealed in Ag–Pd capsules with fluids of various nature, including pure distilled water, 0.5 m NaCl solution, and 10% HF acid. The experiments were conducted at temperatures as low as 150°C under P_f = 0.5 to 3.5 kbar for a duration as long as four months. In all cases, stolzite grew at the expense of raspite. Even for the charge with oxide mix and raspite seeds, stolzite was still the final product. It appears from these experi-

ments, that raspite may not have its own *P–T* stability field and may have grown metastably due to unknown kinetic effects.

Discussion and Conclusion

The gradual widening of the miscibility gap with decreasing temperatures in the Ca–Pb series may provide valuable geothermometry by determining the compositions of coexisting scheelite and stolzite. As Pb has a strong affinity for S to form sulfide (galena), rather than tungstate even in the presence of tungsten, stolzite seldom occurs in high-temperature ore deposits where f_{S_2} is usually high. In nature, Mo is readily incorporated into the Ca–Pb series as a substituent for W. However, this can happen only under low f_{S_2} and/or high f_{O_2} conditions (Hsu, 1977)—the same environment where stolzite occurs. A complete solid solution exists between $CaWO_4$ and $CaMoO_4$ to very low temperatures (Hsu and Galli, 1973); this is probably also true between $PbWO_4$ and $PbMoO_4$. Therefore, the effect of minor Mo on the miscibility gap between $CaWO_4$ and $PbWO_4$ may be negligible. Calculation based on Urusov's method to be described below, however, indicates that the theoretical crest temperature of the solvus is about 350°C

Table 3. Run data for the Mn–Zn system

Run No.	Starting Material	T°C	Duration (days)	Run Product Δ2Θ (degrees)*
9Mn1Zn2	Oxide mix	900	4	single solid soln. Δ2Θ = 2.760
9Mn1Zn1	"	400	78	single solid soln.
8Mn2Zn2	"	900	4	single solid soln. Δ2Θ = 2.620
8Mn2Zn1	"	400	148	single solid soln. Δ2Θ = 2.615
7Mn3Zn2	"	900	4	single solid soln. Δ2Θ = 2.470
7Mn3Zn1	"	400	148	single solid soln. Δ2Θ = 2.465
6Mn4Zn2	"	900	6	single solid soln. Δ2Θ = 2.310
6Mn4Zn1	"	400	78	single solid soln.
5Mn5Zn2	"	900	10	single solid soln. Δ2Θ = 2.165
5Mn5Zn6	5Mn5Zn2	700	12	single solid soln.
5Mn5Zn16	Oxide mix	650	110	"
5Mn5Zn5	5Mn5Zn2	600	35	"
5Mn5Zn13	Oxide mix	550	142	"
5Mn5Zn10	"	450	180	"
5Mn5Zn1	"	400	188	single solid soln. Δ2Θ = 2.175
4Mn6Zn2	"	900	6	single solid soln. Δ2Θ = 2.020
4Mn6Zn1	"	400	78	single solid soln.
3Mn7Zn2	"	900	4	single solid soln. Δ2Θ = 1.855
3Mn7Zn1	"	400	160	single solid soln. Δ2Θ = 1.860
2Mn8Zn2	"	900	4	single solid soln. Δ2Θ = 1.705
2Mn8Zn1	"	400	160	single solid soln.
1Mn9Zn2	"	900	4	single solid soln. Δ2Θ = 1.570
1Mn9Zn1	"	400	78	single solid soln.

*Δ2Θ FeKα (102 of quartz and 200 of Mn–Zn) for pure Mn = 2.920°; for pure Zn = 1.435°
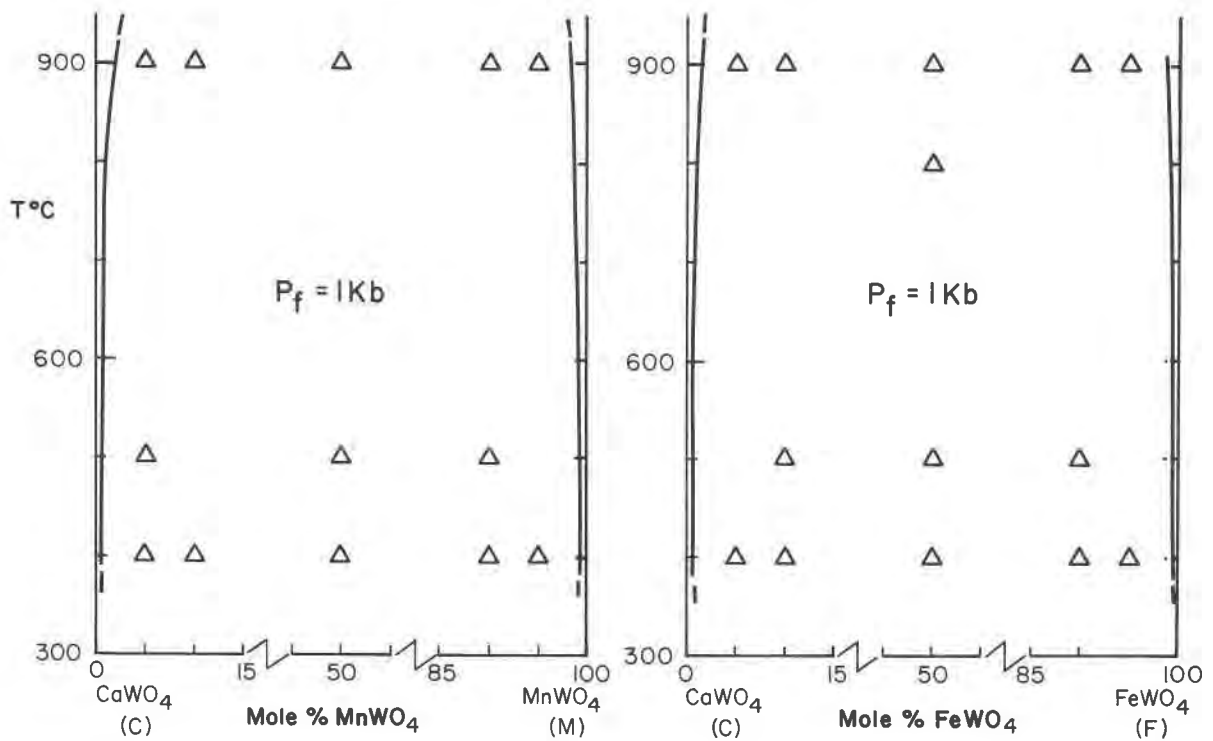
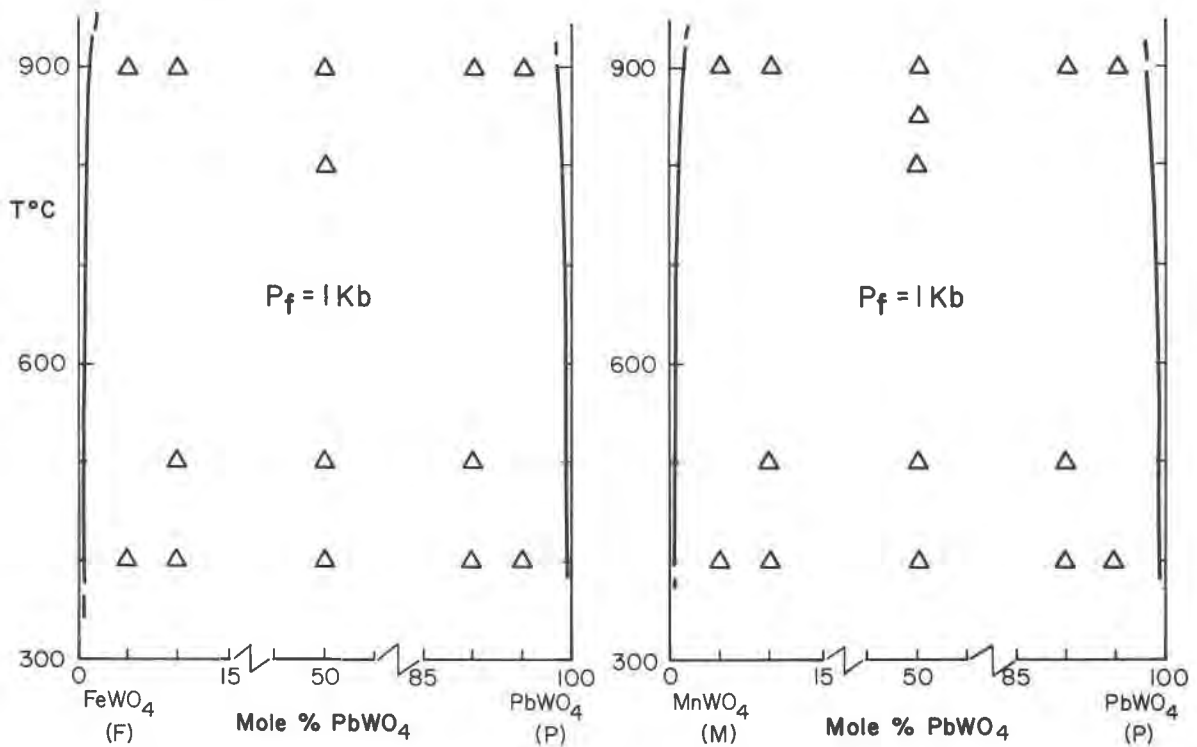Figure 4. T-X diagrams at $P_f = 1.0$ kbar for the Ca-Fe and Ca-Mn systems. Symbols as for Figure 1.

Figure 5. T-X diagrams at $P_f = 1.0$ kbar for the Fe-Pb and Mn-Pb systems. Symbols as for Figure 1.
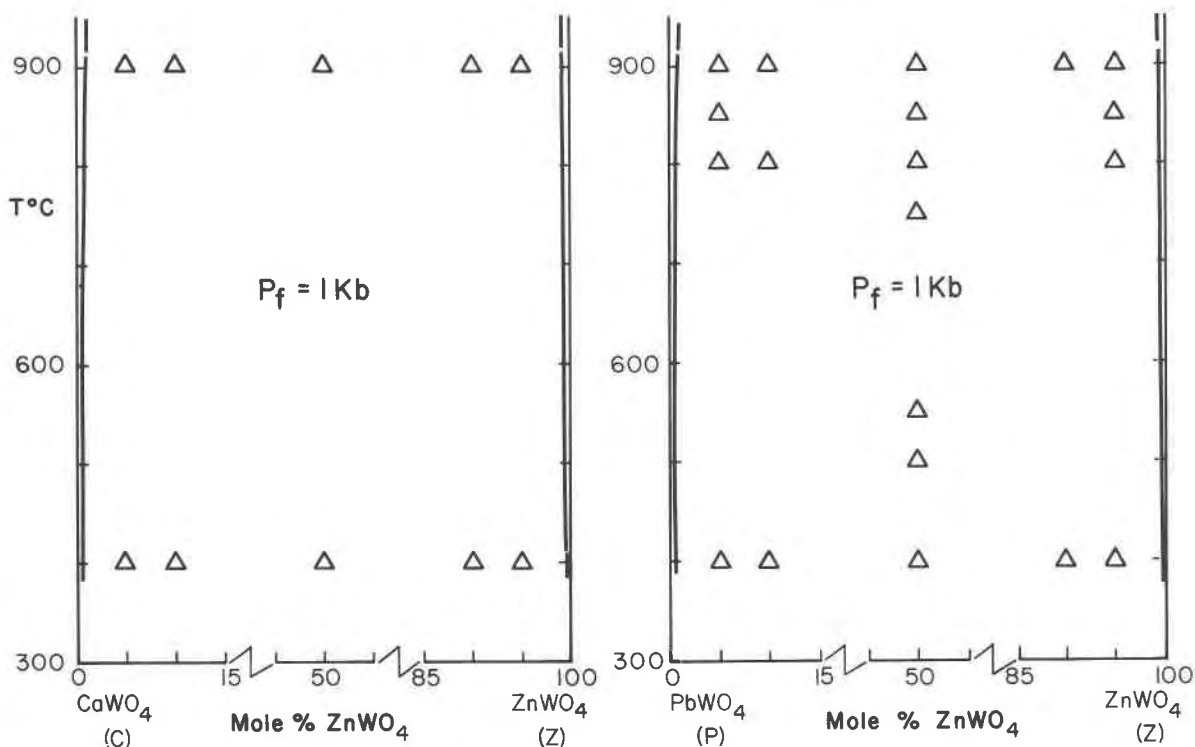
Figure 6. T-X diagrams at $P_f = 1.0$ kbar for the Ca-Zn and Pb-Zn systems. Symbols as for Figure 1.

below the experimentally-determined value of 725°C.

According to Urusov (1975) the absolute maximum temperature of exsolution, T, in a binary system M_kX_1, may be determined by the equation $T =$

Table 4. Run data for the Ca–Fe and Ca–Mn systems

Run No.	Starting Material	T°C	Duration (days)	Run Product Δ2θ (degrees)*
95Ca05Fe2	Oxide mix	900	3	Ca: Δ2θ = 0.945 trace Fe and WO₃
95Ca05Fe1	"	400	71	Ca, trace Fe
9Ca1Fe2	"	900	2	Ca: Δ2θ = 0.945 minor Fe, trace WO₃
9Ca1Fe1	"	400	71	Ca, minor Fe
5Ca5Fe2	"	900	6	Ca: Δ2θ = 0.955 Fe: Δ2θ = 0.640
5Ca5Fe3	"	500	115	Ca,Fe
1Ca9Fe2	"	900	2	Fe: Δ2θ = 0.665 minor Ca
05Ca95Fe2	"	900	3	Fe: Δ2θ = 0.665 trace Ca
05Ca95Fe1	"	400	71	Fe, trace Ca
95Ca95Mn2	Oxide mix	900	3	Ca: Δ2θ = 0.995 trace Mn, trace WO₃
95Ca05Mn1	"	400	78	Ca, trace Mn
9Ca1Mn2	"	900	2	Ca: Δ2θ = 0.990 minor F, trace WO₃
9Ca1Mn1	"	400	78	Ca, minor Mn
5Ca5Mn2	"	900	6	Ca: Δ2θ = 0.995 Mn: Δ2θ = 1.690
5Ca5Mn3	"	500	115	Ca, Mn
1Ca9Mn2	"	900	2	Mn: Δ2θ = 1.695 minor Ca
1Ca9Mn1	"	400	78	Mn, minor Ca
05Ca95Mn2	"	900	3	Mn: Δ2θ = 1.705 trace Ca
05Ca95Mn1	"	400	78	Mn, trace C

*Δ2θ FeKα(111 of Al and 211 of Ca,111 of Al and 200 of Fe or Mn) for pure Ca = 0.953°; for pure Fe = 0.655°; for pure Mn = 1.655°

$c \cdot z_M \cdot z_X \cdot n \cdot m \cdot (\Delta r/d_1)^2/2R$; where c is an empirical parameter and equals 25,000 cal/mol for oxides; z_M and z_X are formal charges (valences) of M and X, respectively; m is the number of atoms in the formula of compound (m = k + 1); n is the coordination number of the cation; Δr is the difference of radii of the substituents; d_1 is the smaller average interatomic distance; and R is the universal gas constant. Using the structure data of monoclinic tungstates listed in Table 3 of Weitzel (1976) and those of tetragonal tungstates by Plakhov et al. (1970), and the ionic radius data of Whittaker and Muntus (1970), the absolute maximum temperatures of unmixing of binary solid solutions are calculated as following:

For Fe–Mn (monoclinic)

$$T = 25,000 \cdot 2 \cdot 2 \cdot 2 \cdot 6 \cdot (0.05/3.973)^2/2 \cdot 1.987$$
$$= 48 \text{ K} = -225°C$$

For Fe–Zn (monoclinic)

$$T = 25,000 \cdot 2 \cdot 2 \cdot 2 \cdot 6 \cdot (0.03/3.947)^2/2 \cdot 1.987$$
$$= 17 \text{ K} = -256°C$$

For Mn–Zn (monoclinic)

$$T = 25,000 \cdot 2 \cdot 2 \cdot 2 \cdot 6 \cdot (0.08/3.947)^2/2 \cdot 1.987$$
$$= 124 \text{ K} = -149°C$$

Table 5. Run data for the Fe–Pb and Mn–Pb systems

Run No.	Starting Material	T°C	Duration (days)	Run Product Δ2θ (degrees)*
95Fe05Pb2	Oxide mix	900	4	Fe: Δ2θ = 0.790
				trace Pb
9Fe1Pb2	"	900	6	Fe, minor Pb
9Fe1Pb3	"	500	40	Fe: Δ2θ = 0.795
				minor Pb
9Fe1P1	"	400	65	Fe, minor Pb
5Fe5Pb2	"	900	7	Pb: Δ2θ = 0.960
				Fe: Δ2θ = 0.795
5Fe5Pb1	"	400	133	Pb: Δ2θ = 0.950
				Fe: Δ2θ = 0.805
1Fe9Pb2	"	900	6	Pb: Δ2θ = 0.960
				minor Fe
1Fe9Pb1	"	400	65	Pb, minor Fe
05Fe95Pb2	"	900	4	Pb: Δ2θ = 0.965
				trace Fe
95Mn05Pb2	Oxide mix	900	4	Mn: Δ2θ = 1.320
				trace Pb
9Mn1Pb2	"	900	6	Mn: Δ2θ = 1.320
				Pb: Δ2θ = 0.980
9Mn1Pb1	"	400	65	Mn: Δ2θ = 1.315
				Pb: Δ2θ = 0.955
5Mn5Pb2	"	900	7	Pb: Δ2θ = 0.978
				Mn Δ2θ = 1.320
5Mn5Pb1	"	400	65	Pb: Δ2θ = 0.970
				Mn: Δ2θ = 1.315
1Mn9Pb2	"	900	4	Pb: Δ2θ = 0.970
				minor Mn
1Mn9Pb1	"	400	65	Pb: Δ2θ = 0.960
				trace Mn
05Mn95Pb2	"	900	4	Pb: Δ2θ = 0.980
				trace Mn

*Δ2θ CuKα(211 of rutile and 312 of Pb, 211 of rutile and 202 of Fe or Mn) for pure Fe = 0.810°; for pure Mn = 1.315°; for pure Pb = 0.955°

For Ca–Pb (tetragonal)

$$T = 25,000 \cdot 2 \cdot 2 \cdot 2 \cdot 8 \cdot (0.17/4.263)^2/2 \cdot 1.987$$

$$= 640 \text{ K} = 367°C$$

Thus, even if a similar degree of discrepancy between theoretical and experimental values of unmixing temperature is assumed in monoclinic tungstates as in tetragonal tungstates, the formation of solid solutions among Fe, Mn, and Zn tungstates down to

Table 6. Run data for the Ca–Zn and Pb–Zn systems

Run No.	Starting Material	T°C	Duration (days)	Run Products Δ2θ (degrees)*
95Ca05Zn2	Oxide mix	900	4	Ca: Δ2θ = 0.480
				trace Zn
9Ca1Zn2	"	900	4	Ca: Δ2θ = 0.480
				trace Zn
5Ca5Zn2	"	900	4	Ca: Δ2θ = 0.480
				Zn: Δ2θ = 1.117
05Ca95Zn2	"	900	4	Zn: Δ2θ = 1.120
				trace Ca
95Pb05Zn7	Tungstate mix	850	4	Pb: Δ2θ = 3.390
				trace Zn
9Pb1Zn2	"	900	4	Pb: Δ2θ = 3.385
				minor Zn
5Pb5Zn2	"	900	4	Pb: Δ2θ = 3.385
				Zn: Δ2θ = 1.120
5Pb5Zn6	"	700	10	Pb: Δ2θ = 3.395
				Zn: Δ2θ = 1.115
5Pb5Zn1	"	400	133	Pb: Δ2θ = 3.400
				Zn: Δ2θ = 1.115
1Pb9Zn2	"	900	4	Zn: Δ2θ = 1.120
				minor Pb
05Pb95Zn7	"	850	4	Zn: Δ2θ = 1.150
				trace Pb

*Δ2θ CuKα(211 of quartz and 224 of Ca and Pb) for pure Ca = 0.490°; for pure Pb = 3.400. Δ2θ CuKα(102 of quartz and 200 of Zn) for pure Zn = 1.110°

400°C or below is to be expected on the basis of this theoretical calculation. Yet, in nature, Fe–Mn is the only system which is found to form a complete solid solution (wolframite). In spite of the constant presence of zinc in most wolframite deposits, $ZnWO_4$ is not only absent from them in pure form but also seldom present as an isomorphous component in wolframite, although some analyses of sanmartinite indicate that up to 46 mole percent $FeWO_4$ may be incorporated in this mineral (Dunn, 1978). This may be attributed to two properties of zinc: (1) Based on geometrical considerations the ionic radius of zinc dictates that six-fold coordination is the stable one for Zn^{2+} ion. Yet zinc has a pronounced tendency to form covalent, tetrahedrally-directed bonds even with oxygen. Indeed, smithsonite, $ZnCO_3$, is the only common zinc mineral with six-fold coordination of Zn^{2+} (Neumann, 1960). (2) Zinc has a stronger affinity for sulfur than iron and manganese (e.g., Marakushev and Bezmen, 1969) and forms sulfide minerals such as sphalerite and wurtzite. Hence the occurrence of $ZnWO_4$ either in its pure form or as an isomorphous component in wolframite requires a rather unusual geologic environment; that is, in the presence of tungsten high f_{O_2} and low f_{S_2}, or sufficient to say, low f_{H_2S} in the presence of water (e.g., Burt, 1977, 1980).

Experimental results, both dry and hydrothermal, indicate that mutual solid solubilities are extremely low even at high temperatures for binary tungstates with different crystal structures as end members. These results appear to be in contradiction to the observation made by Grubb (1967) on the zoned ferberitic wolframite with scheelite exsolution. If the scheelite lamellae within the zoned wolframite are indeed of exsolution rather than replacement origin, three possibilities may be considered: (1) an unreasonably long time is required to attain any degree of solid solution in the laboratory due to unknown kinetic problems, (2) exsolution takes place so fast in the laboratory that any solid solution attained at high temperatures cannot be quenched to room temperature, and/or (3) a metastable solid solution forms in nature (due possibly to very rapid crystal growth) with later exsolution observed by Grubb. Prolonged run durations or high temperature X-ray apparatus is needed to test these possibilities.

The ionic radii and electronegativities of the cations involved in the study are listed in Table 7. The extensive solid solutions among the three monoclinic tungstates and between the two tetragonal tungstates are explained in terms of similarities in these two

Table 7. Ionic radii and electronegativities of some divalent cations

		Pb^{2+}	Ca^{2+}	Mn^{2+}	Fe^{2+}	Zn^{2+}
r^{VI}	(Å)	1.26	1.08	0.91	0.86	0.83
r^{VIII}	(Å)	1.37	1.20	1.01	—	—
E	$(\frac{Kcal}{g \cdot atom})$	170	137	170	200	208

Roman numerals represent coordination numbers. Ionic radius (r) data from Whittaker and Muntus (1970). Electronegativity (E) data from Povarenykh (1964).

quantities. However, if ionic radius and electronegativity are the only controlling factors, extensive solid solution between Ca- and Mn-tungstates, at least as extensive as that between Ca- and Pb-tungstates, should be expected. Indeed, complete solid solutions between Ca- and Mn-end members are often observed in silicate minerals, *e.g.*, between grossular and spessartine (Hsu, 1980). Yet, as experimentally demonstrated, the mutual substitution between Ca^{2+} and Mn^{2+}, not to mention between Ca^{2+} and Fe^{2+}, is extremely limited in the tungstates. Here the host crystal structure appears to play an important role. Figure 7 shows the crystal structures of tetragonal

(A) and monoclinic (B) tungstates. In the tetragonal tungstate structure, the tungsten cations (W^{6+}) are coordinated by four oxygen ions and the divalent cations (Ca^{2+} or Pb^{2+}), by eight. Each oxygen ion, in turn, is surrounded by one W^{6+} and two divalent cations. In the monoclinic tungstate structure, on the other hand, both the hexavalent and divalent cations (Mn^{2+}, Fe^{2+} or Zn^{2+}) are coordinated by six oxygen ions. There are, however, two different oxygens in this structure; one oxygen is surrounded by two W^{6+} and one divalent cation, the other, by one W^{6+} and two divalent cations. These differences in environment, not only for the divalent cations but also for the other ions, may serve to prevent any extensive solid solution.

Acknowledgments

References

Burt, D. M. (1977) Chalcophile-lithophile tendencies in the helvite group: genthelvite stability in the system $ZnO-BeO-Al_2O_3-$
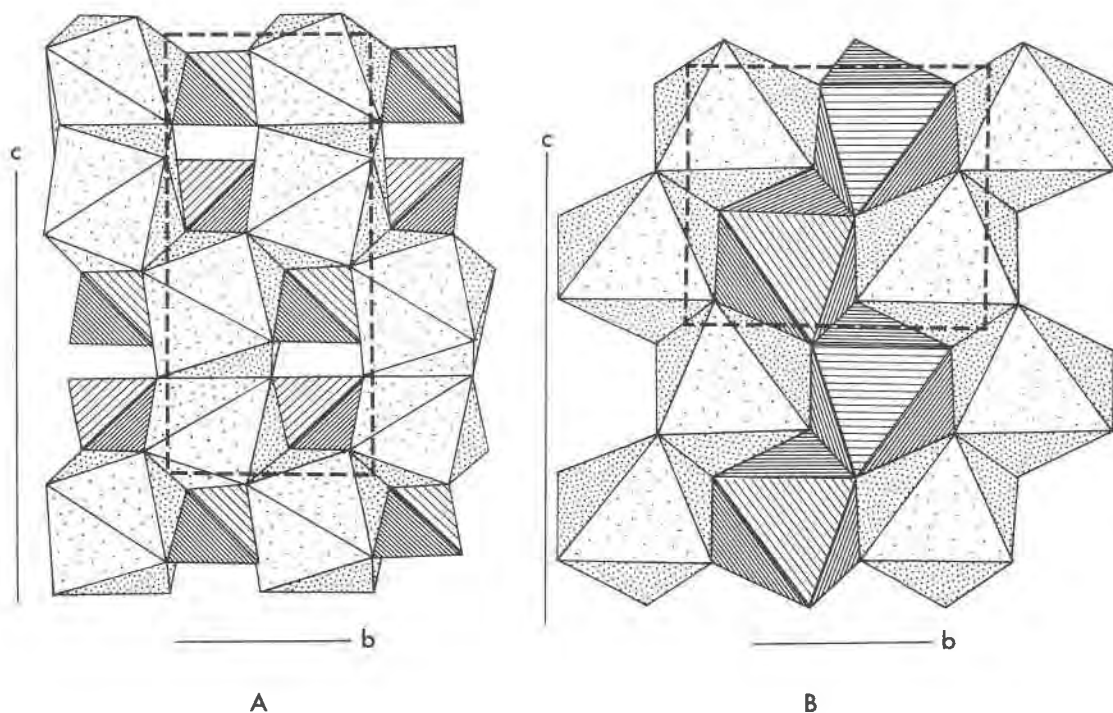

Figure 7. The structures of the tetragonal (A, after Plakhov *et al*, 1970) and monoclinic (B, after Cid-Dresdner and Escobar, 1968) tungstates.

SiO_2–SO_{-1}–F_2O_{-1}. (abstr.) American Geophysical Union Transactions, 58, 1242.

Burt, D. M. (1980) The stability of danalite, $Fe_4Be_3(SiO_4)_3S$. American Mineralogist, 65, 355–360.

Chang, L. L. Y. (1967) Solid solutions of scheelite with other $R^{II}WO_4$–type tungstates. American Mineralogist, 52, 427–435.

Chang, L. L. Y. (1968) Subsolidus phase relations in the system $ZnWO_4$–$ZnMoO_4$–$MnWO_4$–$MnMoO_4$. Mineralogical Magazine, 36, 992–996.

Chang, L. L. Y. (1971) Phase relations in the system PbO–WO_3. Journal of American Ceramic Society, 54, 357–358.

Chernyshev, L. V., Belykh, L. A., and Pastushkova, T. M. (1976) An investigation of solid solutions in the system $FeWO_4$–$MnWO_4$–$ZnWO_4$. Geokhimiya, 5, 716–727 (transl. Geochemistry International, 3, 60–69, 1976).

Cid-Dresdner, H. and Escobar, C. (1968) The crystal structure of ferberite, $FeWO_4$. Zeitschrift für Kristallographie, 127, 61–72.

Dunn, P. J. (1978) Sanmartinite: new data. Mineralogical Magazine, 42, 281.

Fujita, T., Kawada, I. and Kato, K. (1977) Raspite from Broken Hill. Acta Crystallographica, B33, 162–164.

Grubb, P. L. C. (1967) Solid solution relationships between wolframite and scheelite. American Mineralogist, 52, 418–426.

Hsu, L. C. (1976) The stability relations of the wolframite series. American Mineralogist, 61, 944–955.

Hsu, L. C. (1977) Effects of oxygen and sulfur fugacities on the scheelite–tungstenite and powellite–molybdenite stability relations. Economic Geology, 72, 664–670.

Hsu, L. C. (1980) Hydration and phase relations of grossular-spessartine garnets at P_{H_2O} = 2 kb. Contributions to Mineralogy and Petrology, 71, 407–415.

Hsu, L. C. and Galli, P. E. (1973) Origin of the scheelite-powellite series of minerals. Economic Geology, 68, 681–696.

Marakushev, A. A. and Bezmen, N. I. (1969) Chemical affinity of metals for oxygen and sulfur. Geologiya Rudnykh Mestorozh-

denii, 1969, No. 4, 8–23 (transl. International Geology Review, 13, 1781–1794, 1971).

McColl, D. H. (1974) A new occurrence of raspite at the Cordilleran mine, New South Wales, Australia. Australia Gems and Crafts Magazine, 9–11.

Neumann, H. (1960) Notes on the mineralogy and geochemistry of zinc. Mineralogical Magazine, 28, 575–581.

Plakhov, G. F., Pobedimskaya, E. A., Simonov, M. A., and Belov, N. V. (1970) The crystal structure of $PbWO_4$. Kristallografiya, 15, 1067–1068 (transl. Soviet Physics-Crystallography, 15, 928–929, 1971).

Povarennykh, A. S. (1964) Some fundamental problems of crystal chemistry in relation to mineralogy, In M. H. Battey and S. I. Tomkeieff, Eds., Aspects of Theoretical Mineralogy in the U.S.S.R. p. 135–169. MacMillan, New York.

Richter, P. W., Krugger, C. J. and Pistorius, W. F. T. (1976) $PbWO_4$–III (a high-pressure form). Acta Crystallographica, B32, 928–929.

Shaw, R. and Claringbull, G. F. (1955) X-ray study of raspite (monoclinic $PbWO_4$). (abstr.) American Mineralogist, 40, 933.

Shoji, T. (1978) Fluorescent color and x-ray powder data of synthesized scheelite-powellite series as guides to determine its composition. Mining Geology, 28, 397–404.

Tuttle, O. F. (1949) Two pressure vessels for silicate-water studies. Geological Society of America Bulletin, 60, 1727–1729.

Urusov, V. S. (1975) Energetic theory of miscibility gaps in mineral solid solutions. Fortschritte der Mineralogie, 52, 141–150.

Weitzel, H. (1976) Kristallstrukturverfeinerung von Wolframiten und Columbiten. Zeitschritf für Kristallographie, 144, 238–258.

Whittaker, E. J. W. and Muntus, R. (1970) Ionic radii for use in geochemistry. Geochimica et Cosmochimica Acta, 34, 945–956.